



This is a repository copy of *The linear-elastic Theory of Critical Distances to estimate high-cycle fatigue strength of notched metallic materials at elevated temperatures.*

White Rose Research Online URL for this paper:
<http://eprints.whiterose.ac.uk/102868/>

Version: Accepted Version

Article:

Louks, R. and Susmel, L. orcid.org/0000-0001-7753-9176 (2015) The linear-elastic Theory of Critical Distances to estimate high-cycle fatigue strength of notched metallic materials at elevated temperatures. *Fatigue and Fracture of Engineering Materials and Structures*, 38 (6). pp. 629-640. ISSN 8756-758X

<https://doi.org/10.1111/ffe.12273>

This is the peer reviewed version of the following article: Louks, R., and Susmel, L. (2015), The linear-elastic Theory of Critical Distances to estimate high-cycle fatigue strength of notched metallic materials at elevated temperatures. *Fatigue Fract Engng Mater Struct*, 38: 629–640, which has been published in final form at <http://dx.doi.org/10.1111/ffe.12273>. This article may be used for non-commercial purposes in accordance with Wiley Terms and Conditions for Self-Archiving.

Reuse

Unless indicated otherwise, fulltext items are protected by copyright with all rights reserved. The copyright exception in section 29 of the Copyright, Designs and Patents Act 1988 allows the making of a single copy solely for the purpose of non-commercial research or private study within the limits of fair dealing. The publisher or other rights-holder may allow further reproduction and re-use of this version - refer to the White Rose Research Online record for this item. Where records identify the publisher as the copyright holder, users can verify any specific terms of use on the publisher's website.

Takedown

If you consider content in White Rose Research Online to be in breach of UK law, please notify us by emailing eprints@whiterose.ac.uk including the URL of the record and the reason for the withdrawal request.



eprints@whiterose.ac.uk
<https://eprints.whiterose.ac.uk/>

The linear-elastic Theory of Critical Distances to estimate high-cycle fatigue strength of notched metallic materials at elevated temperatures

Richard Louks and Luca Susmel

Department of Civil and Structural Engineering, The University of Sheffield,
Sheffield S1 3JD, United Kingdom

ABSTRACT

This paper investigates the accuracy of the linear-elastic Theory of Critical Distances (TCD) in estimating high-cycle fatigue strength of notched metallic materials experiencing elevated temperatures during in-service operations. The TCD postulates that the fatigue damage extent can be estimated by directly post-processing the entire linear-elastic stress field acting on the material in the vicinity of the crack initiation locations. The key feature of this theory is that the high-cycle fatigue assessment is based on a scale length parameter which is assumed to be a material property. The accuracy of this design method was checked against a number of experimental results generated under axial loading by testing, at 250°C, notched specimens of carbon steel C45. To further investigate the reliability of the TCD, its accuracy was also checked via several data taken from the literature, these experimental results being generated by testing notched samples of Inconel 718 at 500°C as well as notched specimens of directionally solidified superalloy DZ125 at 850°C. This validation exercise allowed us to prove that the linear-elastic TCD is successful in estimating high-cycle fatigue strength of notched metallic materials exposed to elevated temperature, resulting in estimates falling within an error interval of $\pm 20\%$. Such a high level of accuracy suggests that, in situations of practical interest, reliable high-cycle fatigue assessment can be performed without the need for taking into account those non-linearities characterising the mechanical behaviour of metallic materials at high temperature, the used critical distance being still a material property whose value does not depend on the sharpness of the notch being designed.

Keywords: Theory of Critical Distances, notch endurance limit, high temperature

NOMENCLATURE

E	Young's modulus
k	Negative inverse slope
K_t	Stress concentration factor referred to the net area
L	Critical distance value
N_{Ref}	Reference number of cycles to failure in the high-cycle fatigue regime
N_f	Number of cycles to failure
O _{xyz}	System of coordinates
P_S	Probability of survival
r, θ	Polar coordinates
r_n	Notch root radius
R	Load ratio ($R = \sigma_{min} / \sigma_{max}$)
T	Temperature
T_σ	Scatter ratio of the endurance limit range for 90% and 10% probabilities of survival
d_n, w_n	Net diameter/ width
d_g, w_g	Gross diameter/ width
σ_{UTS}	Ultimate tensile strength
ΔK_{th}	Range of the threshold value of the stress intensity factor
$\Delta\sigma_0$	Range of the plain and notch endurance limit extrapolated at N_{Ref} cycles to failure
$\Delta\sigma_1$	Range of the maximum principal stress
$\Delta\sigma_{eff}$	Range of the effective stress
$\Delta\sigma_{net}$	Range of the nominal stress referred to the net area
$\Delta\sigma_{UTS}$	Range of the stress breaking the plain specimens at 1/4 cycles to failure.
$\Delta\sigma_y$	Range of the local stress perpendicular to the notch bisector

INTRODUCTION

Owing to its intrinsic complexity, the fatigue behaviour of metallic materials experiencing elevated temperatures is always a matter of concern to structural engineers engaged in designing real components. The importance of being able to properly and accurately perform the fatigue assessment of components working under extreme temperature conditions is evidenced by the fact that this design problem is key in relevant industrial sectors such as transportation (for example, the blades of jet engines), energy (for example, nuclear power plants), and metalworking & manufacturing (for example, hot rolling of metals). Accordingly, starting from the pioneering work done by Manson [1] and Coffin [2], since about the middle of the last century [3-5], the scientific international community has made a tremendous effort in order to understand/model the mechanical behaviour as well as to predict lifetime of metallic materials subjected, at elevated temperatures, to time-variable load histories. Examination of the state of the art [6] suggests that such an intractable problem has been addressed mainly in terms of strain, the plastic part of the

total cyclic deformation being assumed to play a primary role in those processes resulting, at elevated temperatures, in the initiation of fatigue cracks.

Owing to the fact that real components have complex geometries, numerous experimental/theoretical investigations have been carried out also to quantify the effect of stress/strain concentrators on the overall fatigue behaviour of metallic materials experiencing high in-service temperatures (see, for instance, Refs [7-13] and references reported therein). In this context, due to the important role played by single-crystal metallic materials in the energy sector, also the effect of stress/strain raisers on the high-temperature fatigue strength of single-crystal components have been studied in depth (see, for instance, Refs [14, 15] and references reported therein).

As recently pointed out by Berto, Lazzarin, and Gallo [16], the high-temperature notch fatigue problem has been investigated mainly considering the low/medium-cycle fatigue regime. On the contrary, little research work has been carried out so far in order to formalise and validate appropriate design methods suitable for designing against high-cycle fatigue notched metallic components experiencing high temperatures during in-service operations. In this context, toward the end of the 90s, Nisitani and co-workers [17, 18] have shown that, also at elevated temperatures, the high-cycle fatigue strength of notched specimens of Inconel 718 could successfully be estimated via conventional linear-elastic notch mechanics, the small-yielding conditions being satisfied for this specific material also at 300, 500, and 600°C. By performing an accurate experimental investigation, Shi et al. [19] observed that the fatigue strength at 850°C of notched DZ125 decreases as the linear-elastic stress concentration factor, K_t , increases, K_t being seen to affect also the ratcheting behaviour of this directionally solidified superalloy. By testing plain and notched samples of 40CrMoV13.9 as well as of a copper-cobalt-beryllium alloy, Berto, Lazzarin, and Gallo [16, 20] have proven that, given the material, the strain energy density parameter is capable of summarising in the same scatter band experimental results generated at different temperatures.

As far as room temperature notch fatigue is concerned, it is generally recognised that the so-called Theory of Critical Distances (TCD) [21, 22] is a reliable engineering tool allowing notched components to accurately be designed against high-cycle fatigue. By post-processing a very large number of experimental results [23-25], it has been proven that the TCD is capable of estimates

falling within an error interval of $\pm 20\%$, such a high accuracy level being reached also under multiaxial fatigue loading [26-30]. According to the TCD's *modus operandi*, notch fatigue strength is estimated via an effective stress whose definition depends on a material critical length, the stress analysis being performed by adopting a simple linear-elastic constitutive law. According to the most general formulation of the TCD, such a theory makes use of a length scale parameter which is treated as a material property, i.e., its value is assumed not to vary as the sharpness of the assessed notch changes.

Turning back to the high-temperature notch fatigue issue, Yang et al. [31] have recently investigated the accuracy of the TCD in estimating fatigue damage in notched specimens of directionally solidified superalloy DZ125 subjected, at 850°C , to axial fatigue loading. In this study the TCD was applied by considering not only the linear-elastic [21, 22] but also the elasto-plastic [32] formalisation of this theory. By post-processing their experimental results according to a particular re-interpretation of the above strategies, the authors came to the conclusion that, for the specific superalloy being tested, the critical distance value was somehow affected by the notch sharpness. It is worth recalling here also that Leidermark et al. [33] have recently shown that the critical plane method applied along with the critical distance concept can successfully be used to estimate lifetime of notched single-crystal superalloy MD2 subjected, at 500°C , to uniaxial fatigue loading.

In this complex scenario, the aim of the present paper is to investigate whether the linear-elastic TCD is successful in estimating high-cycle fatigue strength of notched metallic materials also at elevated temperatures, the length scale parameter being still treated as a material property whose value does not depend on the notch sharpness.

FUNDAMENTALS OF THE THEORY OF CRITICAL DISTANCES

According to the TCD's *modus operandi*, high-cycle notch fatigue strength is directly estimated by post-processing the entire stress field acting on the material in the vicinity of the stress raisers being assessed [22]. One of the most remarkable features of the TCD is that this theory is capable of accommodating those non-linearities characterising the mechanical behaviour of ductile metallic materials into a linear-elastic framework, this holding true not only in the high-cycle [24], but also

in the medium-cycle fatigue regime [34]. Accordingly, the stress analysis can directly be performed by assuming that metallic materials obey a simple linear-elastic constitutive law. This obviously results in a great simplification of the fatigue assessment problem, allowing the time and costs of the design process to be reduced considerably [35].

To perform the high-cycle fatigue assessment of notched components, the TCD makes use of the range of an effective stress, $\Delta\sigma_{\text{eff}}$, which is calculated by taking into account a suitable material length scale parameter. In this context, such a critical distance is assumed to be a material property whose value can directly be determined via appropriate experiments run by using standard testing equipment [36]. The TCD can be formalised in different ways which include the Point Method (PM) [37], the Line Method (LM) [38], and the Area Method [39]. In particular, when the TCD is applied in the form of the PM, $\Delta\sigma_{\text{eff}}$ is estimated at a certain distance from the apex of the stress concentrator (Fig. 1b); the LM postulates instead that $\Delta\sigma_{\text{eff}}$ has to be calculated by averaging the linear-elastic stress over a line (Fig. 1c); finally, according to the AM, $\Delta\sigma_{\text{eff}}$ can also be determined by averaging the linear-elastic maximum principal stress over an area (Fig. 1d). According to the symbolism adopted in Fig. 1a, the above definitions of the range of the effective stress, $\Delta\sigma_{\text{eff}}$, can be formalised mathematically as [22]:

$$\Delta\sigma_{\text{eff}} = \Delta\sigma_y \left(\theta = 0, r = \frac{L}{2} \right) \quad (\text{Point Method}) \quad (1)$$

$$\Delta\sigma_{\text{eff}} = \frac{1}{2L} \int_0^{2L} \Delta\sigma_y(\theta = 0, r) dr \quad (\text{Line Method}) \quad (2)$$

$$\Delta\sigma_{\text{eff}} = \frac{4}{\pi L^2} \int_0^{\pi/2} \int_0^L \Delta\sigma_1(\theta, r) \cdot r \cdot dr \cdot d\theta \quad (\text{Area Method}) \quad (3)$$

In Eqs (1) to (3) material characteristic length L is determined via the range of the threshold value of the stress intensity factor, ΔK_{th} , and the plain fatigue limit, $\Delta\sigma_0$, as follows [21, 22, 41]:

$$L = \frac{1}{\pi} \left(\frac{\Delta K_{\text{th}}}{\Delta\sigma_0} \right)^2, \quad (4)$$

It is important to highlight here that, to correctly take into account the mean stress effect in fatigue, the values of both ΔK_{th} and $\Delta\sigma_0$ used to estimate L have to be determined experimentally under the same load ratio, $R=\sigma_{min}/\sigma_{max}$, as the one damaging the component being assessed. Definition (4) should make it evident that, since the critical distance value is a function of two material properties, L is in turn a material property which is seen to be different for different materials and different load ratios.

From a materials science point of view, the fatigue limit in metals corresponds to the initiation of a microstructural crack whose propagation is arrested either by the first grain boundary or by the first micro-structural barrier [42, 43]. Non-ferrous metals instead do not have a fatigue limit, therefore they must always be designed for finite lifetime (for instance, this is the fatigue behaviour which is displayed by aluminium alloys). Under these circumstances, the high-cycle fatigue assessment is performed via the so-called endurance limit. By definition, the endurance limit is the range of the stress extrapolated at a given number of cycles to failure, N_{Ref} (where N_{Ref} is typically taken in the interval $5\cdot 10^5 \div 10^8$ cycles to failure) [44]. In situations of practical interest, many different external factors (elevated temperatures included) can result in the elimination of the fatigue limit also in those metals which potentially have a fatigue limit [45, 46]. Accordingly, when it comes to designing real notched components against high-cycle fatigue, the use of appropriate endurance limits is always advisable [46].

When either the range of the threshold value of the stress intensity factor is not available or the material being designed does not exhibit a fatigue limit, the required critical distance can accurately be determined by using two endurance limits obtained by testing un-notched specimens and samples weakened by a known geometrical feature [34]. The in-field procedure suggested as being followed to determine L according to this strategy is described in Fig. 2. In particular, the S-N chart sketched in Fig. 2a plots two fatigue curves. The upper fatigue curve is assumed to be generated by testing plain specimens, whereas the lower one by testing samples containing a particular geometrical feature. According to the PM, Eq. (1), given the reference number of cycles to failure, N_{Ref} , $L/2$ is the distance from the notch apex at which the range of the linear-elastic local

stress, $\Delta\sigma_y$, equals the stress range, $\Delta\sigma_0$, which has to be applied to the parent material to generate a failure at $N_f=N_{Ref}$ cycles to failure. The required linear-elastic stress field in the vicinity of the stress raiser under the range of the nominal stress, $\Delta\sigma_{net}$, breaking the notched samples at $N_f=N_{Ref}$ cycles to failure (Fig. 2b) can be determined either numerically (i.e., using the Finite Element (FE) method) or through suitable analytical solutions. In the next sections this strategy will be adopted to determine the critical distance value for the materials which will be used to check the accuracy of the linear-elastic TCD in estimating notch endurance limits at elevated temperatures.

Having reviewed the fundamentals of the TCD, it is worth concluding by observing that a notched component is assumed to be at its fatigue/endurance limit as long as the following conditions is assured:

$$\Delta\sigma_{eff} \leq \Delta\sigma_0 \quad (5)$$

where the range of the effective stress, $\Delta\sigma_{eff}$, can be calculated according to either the PM, Eq. (1), the LM, Eq. (2), or the AM, Eq. (3).

EXPERIMENTAL DETAILS

In order to check the accuracy of the linear-elastic TCD in estimating high-cycle fatigue strength of notched metals at elevated temperatures, plain and notched samples of structural steel C45 (similar to SAE 1045) were tested under axial loading at 250° C, the load ratio, R, being set equal to 0.1. Examination of the state of the art suggests that the fatigue behaviour of metallic materials at elevated temperatures has been investigated mainly considering high-performance alloys. This is a consequence of the fact that materials having superior mechanical properties are obviously used in those extreme situations involving time variable loading and elevated temperatures (such as, for instance, the blades of jet engines). However, it has to be said that, there are situations of practical interest where conventional structural steels as well experience medium/high temperatures during in service operations (as it happens, for instance, to the steel structural parts of vehicle engines and engine beds). As to the expected mechanical behaviour at high-temperature of structural steel C45,

by testing under fatigue loading specimens of SAE 1045, Christ et al. [47] have observed that, given the amplitude and mean stress of the loading cycle, fatigue damage reaches its maximum value at a temperature in the range 200-250°C. The reasons briefly summarised above should explain the motivations behind the choice of testing commercial structural steel C45 at 250°C.

The geometries of both the un-notched and notched specimens tested at the Materials Testing Laboratory of the University of Sheffield are sketched in Figure 3. The fatigue tests were performed using a 100kN Mayes fatigue testing machine (Fig. 4) controlled through controller Kelsey Instruments K7500. During testing the temperature inside the furnace was kept constant and equal to 250°C through an external controller connected to a number of thermocouples located inside the furnace itself. Not to alter the magnitude of the applied loading during high-temperature testing, the apparatus was set up so that the loading cell was positioned outside the furnace. Further, the loading cell was continuously kept at room temperature by using an *ad hoc* external cooling system. Figure 4 shows the testing apparatus as well as a plane sample positioned inside the furnace and clamped through the mechanical grips which were specifically designed and manufactured for this type of experimental investigation.

The fatigue tests were performed according to the following experimental protocol. Initially, the fatigue samples were clamped using the mechanical grips as shown in Figure 4. Subsequently, the furnace was switched on allowing the internal temperature to reach 250°C. As soon as the internal temperature was equal to 250°C, the samples were left inside the furnace for at least an hour. Before testing, the furnace was opened and the bolts were tightened to compensate possible thermal dilatations. After tightening the bolts, the samples were left inside the furnace for at least 30 minutes to ensure that the material to be tested was at the correct temperature. It is worth noticing here that during this initial pre-test phase no evident creep/relaxation phenomena were detected.

Fatigue tests were performed, in load control, under a load ratio, R , equal to 0.1 at a frequency of 15 Hz. The failure criterion was the complete breakage of the samples. The picture in Figure 3b displays some examples summarising the cracking behaviour observed both in the plain and in the notched samples.

The experimental results generated by testing the plain and notched specimens shown in Figure 3 are summarised in the Wöhler diagrams of Figure 5. These log-log diagrams plot the range of the nominal net stress, $\Delta\sigma_{\text{net}}$, against the number of cycles to failure, N_f . The charts of Figure 5 report not only the Wöhler curves estimated for a probability of survival, P_s , of 50%, but also the scatter bands calculated for P_s equal to 10% and 90%, respectively. Such fatigue curves were determined by post-processed the data under the hypothesis of a log-normal distribution of the number of cycles to failure for each stress level, the confidence level being taken equal to 95% [48, 49]. The results of the statistical re-analysis are also summarised in Table 1 in terms of negative inverse slope, k , range of the endurance limit (for $P_s=50\%$) extrapolated at $N_{\text{Ref}}=5\cdot 10^5$ cycles to failure, $\Delta\sigma_0$, and scatter ratio of the endurance limit range for 90% and 10% probabilities of survival, T_σ . As suggested by Sonsino [46] for structural steels, the reference number of cycle to failure, N_{Ref} , was taken equal to $5\cdot 10^5$ cycles to failure, the run out data displayed in the charts of Figure 5 confirming the validity of this assumption. To conclude, it is worth pointing out explicitly that, both in Table 1 and in Figure 5, the ranges of the notch endurance limits extrapolated at $N_{\text{Ref}}=5\cdot 10^5$ cycles to failure, $\Delta\sigma_0$, were calculated with respect to the nominal net section.

VALIDATION BY EXPERIMENTAL DATA

In order to check the accuracy of the linear-elastic TCD in estimating the high-cycle fatigue strength of the notched samples of C45 we tested at 250°C, initially attention was focussed on the stress analysis problem. The linear-elastic stress fields in the vicinity of the apices of the investigated stress raisers were estimated by using commercial FE software ANSYS®. The specimens were modelled adopting bi-dimensional elements Plane 183. This 2D element is a higher order 8-node element, having quadratic displacement behaviour. Each node has two degrees of freedom, i.e., translations in the nodal x and y directions. This element can be used as a plane element (plane stress, plane strain and generalized plane strain) or as an axisymmetric element. In order to accurately determine the necessary stress-distance curves, the mesh density in the vicinity of the notch tips was gradually increased until convergence occurred. In particular, the mesh density was gradually increased until profile and magnitude of the determined linear-elastic stress

fields were no longer affected by the mesh density itself. This resulted in elements in the vicinity of the notch tip having size lower than 0.005 mm.

The mechanical clamping devices displayed in Figure 4 were designed so that, during testing, they could rotate about an axis perpendicular to the plane containing the surface of the samples themselves. This allowed the local stress concentration phenomena to be maximised due to the effect of the secondary bending. Owing to the fact that the rotation angles characterising the cyclic movement of the grips during the testing of the notched specimens were seen to be very small, the effect of the secondary bending was modelled in the FE simulations by simply un-constraining the displacements perpendicular to the direction along which the loading was applied. It is also worth pointing out explicitly that this particular way of clamping the samples resulted in no superimposed static torsional stresses.

The FE analyses performed as described above resulted in a net stress concentration factor, K_t , equal to 6.9 for the blunt U-notches, to 10.0 for the sharp U-notches, and, finally, to 26.5 for the sharp V-notches (see also Figure 3 and Table 1).

The critical distance value for the investigated structural steel was determined by using the method summarised in Figure 2. In particular, as shown by the stress vs. distance chart of Figure 6, a critical distance value of 0.252 mm was obtained via the plain endurance limit and the linear-elastic stress field arising, at the endurance limit condition, from the sharp V-notch. This diagram shows also that the linear-elastic PM was highly accurate in estimating the high-cycle fatigue strength of both the bluntly and the sharply U-notched specimens. The error band plotted in Figure 6 was determined by calculating the error as follows:

$$\text{Error} = \frac{\Delta\sigma_{\text{eff}} - \Delta\sigma_0}{\Delta\sigma_0} [\%] \quad (6)$$

where $\Delta\sigma_{\text{eff}}$ is the effective stress calculated according to either the PM, LM, or AM, whereas $\Delta\sigma_0$ is the un-notched material endurance limit.

Table 1 confirms that the TCD used in the form of the PM, LM, and AM was capable of estimates falling within an error interval of $\pm 15\%$, this holding true independently from the sharpness of the

assessed notch. Such a high level of accuracy is very promising because, in general, it is not possible to distinguish between an error of $\pm 20\%$ and an error of 0% due to the problems which are usually encountered during testing as well as during the numerical analyses [36].

In light of the encouraging results obtained when using the linear-elastic TCD to post-process the results we generated by testing, at 250°C , the notched samples of C45, the accuracy and reliability of our design method was further checked against two datasets taken from the literature.

Chen et al. [16] investigated the high-cycle fatigue behaviour of notched cylindrical specimens of Inconel 718. The samples were tested under rotating bending ($R=-1$) at 500°C . As shown in Table 2, the net diameter, w_n , of the samples was kept constant and equal to 8 mm, the gross diameter, w_g , being equal to either 9 mm or 10 mm. Three different values of the notch root radius were investigated, i.e., $r_n=1$ mm, $r_n=0.1$ mm, and $r_n=0.05$ mm.

Shi et al. [19] tested, at 850°C , flat samples with a single lateral notch of directionally solidified superalloy DZ125. The axial cyclic force was applied along a direction parallel to the direction of solidification, the loading rate, R , being kept constant and equal to 0.1. The two considered U-notched geometries had gross width, w_g , equal to 6 mm, net width, w_n , equal to 5.4 mm and 5.5 mm, and root radius, r_n , equal to 0.4 mm and 0.2 mm, respectively. Two series of results generated by testing single V-notched specimens were also considered. The V-notched samples with notch opening angle equal to 60° had $w_g=6$ mm, $w_n=5.5$ mm, and $r_n=0.2$ mm. The V-notched specimens with notch opening angle equal to 120° had instead $w_g=6$ mm, $w_n=5.4$ mm, and $r_n=0.3$ mm. The parent material results were generated by testing, under $R=0.05\div 0.1$, cylindrical samples having diameter equal to 10 mm [50]. Table 3 summarises the considered experimental results in terms of negative inverse slope, k , range of the net endurance limit (for $P_S=50\%$), $\Delta\sigma_0$, and scatter ratio of the endurance limit range for 90% and 10% probabilities of survival, T_σ . Since the experimental results used to determine the above fatigue curves were generated mainly in the range $5\cdot 10^2\div 10^6$ cycles to failure, in order to determine the corresponding endurance limits in a consistent and reliable way, the reference number of cycles to failure, N_{Ref} , was taken equal to 10^6 cycles to failure. From a statistical point of view, the experimental results were post-processed under the hypothesis of a log-normal distribution of the number of cycles to failure for each stress level, the confidence

level being taken equal to 95% [48, 49]. It has to be pointed out here also that those results obtained by testing U- and V-notches with $r_n=0.2$ mm were re-analysed together. This was done to have a population of data enough numerous to be representative from a statistical point of view. In terms of profile of the local linear-elastic stress fields, this simplification resulted just in a little loss of accuracy, since, in the presence of sharp V-notches, the effect of the notch opening angle on the stress distribution is seen to be very little as long as the opening angle itself is lower than 90° [51]. Accordingly, in the validation exercise discussed below, the V-notches having opening angle equal 60° were modelled as U-notches with root radius equal to 0.2 mm.

An interesting aspect highlighted by Table 3 is that, whilst the presence of a notch clearly lowers the overall strength of DZ125 at 850°C , the plain fatigue curve is steeper than the ones obtained by testing notched specimens.

In order to determine the required linear-elastic stress fields, the investigated geometries were modelled using commercial FE software ANSYS®, the mesh density in the vicinity of the stress concentrator apices being gradually increased until convergence occurred. For the sake of completeness, it is worth observing here that the values for the net stress concentration factors estimated according to this standard numerical procedure (see Tables 2 and 3) were slightly different from the corresponding values reported in the original sources [16, 19].

Figure 7 displays the stress-distance curves, at the endurance limit condition, for the notched specimens of Inconel 718 tested by Chen et al. [16]. The value for the critical distance shown in the above chart (i.e., $L=0.154$ mm) was estimated according to the method summarised in Figure 2 by using the plain endurance limit ($\Delta\sigma_0=710$ MPa) and the notch endurance limit experimentally determined by testing the samples having $K_t=8$. The diagram of Figure 7 (see also Table 2) clearly proves that the PM was highly accurate in estimating the high-cycle fatigue strength of the other notched geometries, with estimates falling within an error interval of $\pm 20\%$. Table 2 indicates that a similar level of accuracy was obtained also when the TCD was applied in the form of both the LM and the AM.

The diagram of Figure 8 summarises the stress-distance curves determined by post-processing the experimental results generated by Shi et al. [19] by testing, at 850°C , notched flat samples of

directionally solidified superalloy DZ125. Owing to the numerous assumptions which were made to determine the fatigue curves summarised in Table 3, for this material the length scale parameter was calculated by using the three curves reported in Figure 8. A value of 0.452 mm was obtained for critical distance L by simply adopting a standard best fit procedure. The errors listed in Table 3 prove that the TCD used in the form of the PM, LM, and AM was capable of predictions falling within an error interval of $\pm 20\%$, such a remarkable accuracy being obtained without the need for changing the L value as the sharpness of the assessed notch varied.

To conclude, the error vs. stress concentration factor diagram of Figure 9 summarises the overall level of accuracy which was reached by using the linear-elastic TCD to estimate notch endurance limits at high temperature. This diagram seems to strongly support the idea that, in the presence of notches experiencing in-service elevated temperatures, accurate high-cycle fatigue assessment can be performed not only by continuing to adopt a linear-elastic constitutive law to model the mechanical behaviour of the material being designed, but also by continuing to treat critical distance L as a material property.

The TCD postulates that fatigue assessment has to be performed by post-processing the entire stress field damaging the so-called process zone (i.e., that material portion controlling the overall fatigue strength of the component being designed) [36, 44]. The size of the process zone depends mainly on: (i) material microstructural features, (ii) local micro-mechanical properties, and (iii) nature of the physical mechanisms resulting in the initiation of fatigue cracks [27]. In this setting, by using the AM argument (see Figure 1d), it is possible to presume that the radius defining the size of the process zone approaches critical distance L [27].

Yokobori et al. [52] performed an accurate experimental investigation by testing, at 650°C , V-notched samples of stainless steel SUS304. Their *in situ* observations revealed that, under fatigue loading, damage was localised in a small region in the vicinity of the notch tip, eventually resulting in the initiation of a fatigue crack. The formation of such a highly damaged zone was evidenced by a clear change in the local morphology of the investigated material. This seems to strongly support the idea that, also at elevated temperatures, the TCD is successful in estimating high-cycle notch fatigue strength because the process zone supplies all the engineering information which is required to accurately quantify the effect of those damaging mechanism locally altering the

material morphology. In other words, in contrast to the classic approach [53], the TCD assumes that the fatigue damage extent does not depend solely on the stress state at the tip of the notch being assessed. The TCD postulates instead that the overall fatigue strength of a notched component is controlled by a finite portion of material (having size of the order of L). According to this schematisation, localised stress concentration phenomena (such as surface roughness) play a role of secondary importance due to the fact that, in terms of damaging effect, the stress field perturbation caused by a macroscopic notch prevails over the highly confined perturbation due to superficial asperities. In this context, it is evident that it would be very interesting to check the accuracy of the TCD when the relevant stress fields are determined by explicitly considering not only the effect of macroscopic notches, but also the presence of localised stress concentration phenomena due to surface roughness. This combined approach may explain the reason why in certain materials (such as, for instance, those aluminium alloys commonly used in aircraft construction [54]) a reduced variation of the surface roughness can remarkably affect the total fatigue lifetime.

Another interesting aspect which is worth commenting here is that the TCD estimates high-cycle fatigue strength by directly post-processing the linear-elastic stress fields in the vicinity of the assumed crack initiation locations, even though, within the process zone, the local mechanical behaviour of metallic materials at elevated temperatures is highly non-linear. As to the above aspect, one may argue that the linear-elastic TCD is still successful because, as demonstrated by Lazzarin and Zambardi [55] by using a sophisticated energy argument, the linear-elastic energy equals the elasto-plastic one, when they are averaged over the entire fatigue process zone.

Even if the considerations reported above offer an explanation for why the linear-elastic TCD is successful also in performing the high-cycles fatigue assessment of notched metallic materials experiencing elevated temperatures, it is evident that more work needs to be done in this area to more rigorously link the TCD's *modus operandi* to the physical processes taking place within the process zone and resulting in the initiation of fatigue cracks.

CONCLUSIONS

- The linear-elastic TCD applied in the form of the PM, LM, and AM is successful in estimating high-cycle notch fatigue strength of metallic materials at elevated temperatures.
- The TCD allows notched components experiencing in-service high-temperature to be designed against high-cycle fatigue by directly post-processing the relevant stress fields determined through conventional linear-elastic FE models. This implies that an accurate high-cycle fatigue assessment can be performed without the need for explicitly modelling the highly non-linear mechanical behaviour displayed by metallic materials when exposed to elevated temperatures.
- At high-temperature as well, the TCD can be used to design notched components against fatigue by treating the required critical distance as a material property whose value is not affected by the sharpness of the notch being assessed.
- More work needs to be done in this area to coherently extend the use of the stress based linear-elastic TCD to the medium-cycle fatigue regime.

REFERENCES

- [1] Manson, S. S. (1954) Behaviour of Materials Under Conditions of Thermal Stress. *National Advisory Committee for Aeronautics*, Report No. NACA TN-2933.
- [2] Coffin, L. F. (1954) A Study of the Effects of Cyclic Thermal Stresses on a Ductile Metal. *Trans. ASME* **76**, 931–950.
- [3] Carden, A. E., McEvily, A. J., Wells, C. H. (1973) *Fatigue at elevated temperatures*. ASTM Special Technical Publication 520, Philadelphia, Pa. 19103, USA, 1-787.
- [4] Viswanathan, R., (1989) *Damage Mechanisms and Life Assessment of High Temperature Components*. ASM International, USA, ISBN: 0-87170-358-0.
- [5] Verrilli M. J., Castelli, M. J. (1996) *Thermomechanical Fatigue Behavior of Materials: Second volume*. ASTM STP 1263, Philadelphia, USA, 1-373.
- [6] Manson, S. S., Halford, G. R. (2009) *Fatigue and Durability of Metals at High Temperatures*. ASM International, USA, ISBN-13: 978-0-87170-718-5.
- [7] Domas, P.A. and Antolovich, S.D. (1985). An integrated local energy density approach to notch low cycle fatigue life prediction. *Engng. Fract. Mech.* **21**, 187–202.
- [8] Hasebe, T., Sakane, M. and Ohnami, M. (1992). High temperature low cycle fatigue and cyclic constitutive relation of MAR–M247 directionally solidified superalloy. *Trans ASME* **114**, 162–67.
- [9] Inoue T., Sakane M., Fukuda Y., Igari T., Miyahara M., Okazaki, M. (1994) Fatigue-creep life prediction for a notched specimen of 2¼ Cr-1Mo steel at 600 °C. *Nuclear Engineering and Design* **150**, 141 – 149.
- [10] Hurley a, P.J., Whittaker, M.T., Williams, S.J., Evans, W.J. (2008) Prediction of fatigue initiation lives in notched Ti 6246 specimens. *Int. J. Fatigue* **30**, 623–634.
- [11] Nozaki, M., Zhang, S., Sakane, M., Kobayashi, K. (2011) Notch effect on creep–fatigue life for Sn–3.5Ag solder. *Engng. Fract. Mech.* **78**, 1794–1807.

- [12] Ponter, A. R. S., Chen, H., Willis, M. R., Evans, W. J. (2004) Fatigue-creep and plastic collapse of notched bars. *Fatigue Fract. Eng. Mater. Struct.* **27**, 305–318.
- [13] Whittaker, M.T., Evans, W.J., Hurley, P.J., Flynn, D. (2007) Prediction of notched specimen behaviour at ambient and high temperatures in Ti6246. *Int. J. Fatigue* **29**, 1716–1725.
- [14] Filippini, M. (2011) Notched fatigue strength of single crystals at high temperature. *Procedia. Eng.* **10**, 3787–3792.
- [15] Leidermark, D., Moverare, J., Segersäll, M., Simonsson, K., Sjöström, S. and Johansson, S. (2011) Evaluation of fatigue crack initiation in a notched single-crystal superalloy component. *Procedia. Eng.* **10**, 619–24.
- [16] Berto, F., Gallo, P., Lazzarin, P. (2014) High temperature fatigue tests of un-notched and notched specimens made of 40CrMoV13.9 steel. *Materials and Design* **63**, 609–619.
- [16] Chen Q., Kawagoishi N., Nisitani H. (1999) Evaluation of notched fatigue strength at elevated temperature by linear notch mechanics. *Int. J. Fatigue* **21**, 925–931.
- [17] Kawagoishi, N. Chen, Q., Nisitani, H. (2000) Fatigue strength of Inconel 718 at elevated temperatures. *Fatigue Fract. Eng. Mater. Struct.* **23**, 209–216.
- [19] Shi DQ, Hu XA, Wang JK, Yu HC, Yang XG, Huang J. (2013) Effect of notch on fatigue behaviour of a directionally solidified superalloy at high temperature. *Fatigue Fract. Eng. Mater. Struct.* **36**, 1288–1297.
- [20] Berto, F., Lazzarin, Gallo, P. (2014) High-temperature fatigue strength of a copper–cobalt–beryllium alloy. *J Strain Analysis* **49**, 244–256.
- [21] Tanaka K. (1983) Engineering formulae for fatigue strength reduction due to crack-like notches. *International Journal of Fracture* **22**, R39-R46.
- [22] Taylor D. (1999) Geometrical effects in fatigue: a unifying theoretical model. *Int. J. Fatigue* **21**, 413-20.
- [23] Taylor, D., Wang, G. (2000) The validation of some methods of notch fatigue analysis. *Fatigue Fract. Eng. Mater. Struct.* **23**, 387–394.
- [24] Susmel, L., Taylor, D. (2003) Fatigue Design in the Presence of Stress Concentrations. *J. Strain Analysis* **38**, 443-452.
- [25] Susmel, L., Taylor, D., Tovo, R. (2008) On the estimation of notch fatigue limits by using the Theory of Critical Distances: L, a_0 and open notches. *Structural Durability and Health Monitoring* **4**, 1-18.
- [26] Susmel, L., Taylor, D. (2003) Two methods for predicting the multiaxial fatigue limits of sharp notches. *Fatigue Fract. Eng. Mater. Struct.* **26**, 821-833.
- [27] Susmel, L. (2004) A unifying approach to estimate the high-cycle fatigue strength of notched components subjected to both uniaxial and multiaxial cyclic loadings. *Fatigue Fract. Engng. Mater. Struct.* **27**, 391-411.
- [28] Susmel, L., Taylor, D. (2008) The Modified Wöhler Curve Method applied along with the Theory of Critical Distances to estimate finite life of notched components subjected to complex multiaxial loading paths. *Fatigue Fract. Engng. Mater. Struct.* **31**, 1047-1064.
- [29] Susmel L., Taylor, D. (2012) A critical distance/plane method to estimate finite life of notched components under variable amplitude uniaxial/ multiaxial fatigue loading. *Int. J. Fatigue* **38**, 7-24.
- [30] Louks, R., Gerin, B., Draper, J., Askes, H., Susmel, L. (2014) On the multiaxial fatigue assessment of complex three-dimensional stress concentrators. *Int. J. Fatigue* **63**, 12-24, 2014.
- [31] Yang, X., Wang, J., Liu, J. (2011) High temperature LCF life prediction of notched DS Ni-based superalloy using critical distance concept. *Int. J. Fatigue* **33**, 1470–1476.

- [32] Susmel L, Taylor D. (2010) An elasto-plastic reformulation of the theory of critical distances to estimate lifetime of notched components failing in the low/medium-cycle fatigue regime. *Trans. ASME, J. Eng. Mater. Technol.* **132**, 021002-1/8.
- [33] Leidermark, D., Moverare, J., Simonsson, K. and Sjöström, S. (2011). A combined critical plane and critical distance approach for predicting fatigue crack initiation in notched single-crystal superalloy components. *Int. J. Fatigue* **33**, 1351–59.
- [34] Susmel, L., Taylor, D. (2007) A novel formulation of the Theory of Critical Distances to estimate Lifetime of Notched Components in the Medium-Cycle Fatigue Regime. *Fatigue Fract. Engng. Mater. Struct.* **30**, 567-581.
- [35] Susmel, L. (2008) The Theory of Critical Distances: a review of its applications in fatigue. *Eng. Frac. Mech.* **75**, 1706-1724.
- [36] Taylor, D. (2007) *The Theory of Critical Distances: A new perspective in fracture mechanics*. Elsevier, Oxford, UK.
- [37] Peterson, R.E. (1959) Notch Sensitivity. In: *Metal Fatigue*. Edited by G. Sines and J. L. Waisman, New York, McGraw Hill, 293-306.
- [38] Neuber, H. (1958) *Theory of notch stresses: principles for exact calculation of strength with reference to structural form and material*. Springer Verlag, Berlin, II Ed..
- [39] Sheppard, S.D. (1991) Field effects in fatigue crack initiation: long life fatigue strength. *Trans. ASME. Journal of Mechanical Design* **113**, 188-194.
- [40] Lazzarin P., Tovo R., Meneghetti G. (1997) Fatigue crack initiation and propagation phases near notches in metals with low notch sensitivity. *Int. J. Fatigue* **19**, 647–57.
- [41] El Haddad, M.H., Topper, T.H., Smith, K.N. (1979) Fatigue crack propagation of short cracks. *Trans. ASME, J. Engng. Mater. Tech.* **101**, 42-45.
- [42] Miller, K. J. (1993) The two thresholds of fatigue behaviour. *Fatigue Fract. Engng. Mater. Struct.* **16**, 931-939.
- [43] Akiniwa, Y., Tanaka, K., Kimura, H. (2001) Microstructural effects on crack closure and propagation thresholds of small fatigue cracks. *Fatigue Fract. Engng. Mater. Struct.* **24**, 817-829.
- [44] Susmel, L. (2009) *Multiaxial Notch Fatigue: from nominal to local stress-strain quantities*. Woodhead & CRC, Cambridge, UK, ISBN: 1 84569 582 8.
- [45] Miller, K. J., O'Donnell, W. J. (1999) The fatigue limit and its elimination. *Fatigue Fract. Engng. Mater. Struct.* **22**, 545-557.
- [46] Sonsino, C. M. (2007) Course of SN-curves especially in the high-cycle fatigue regime with regard to component design and safety. *Int. J. Fatigue* **29**, 2246–2258.
- [47] Christ, H.-J., Wamukwamba, C.K., Mughrabi, H. (1997) The effect of mean stress on the high-temperature fatigue behaviour of SAE 1045 steel. *Materials Science and Engineering* **A234-236**, 382-385.
- [48] Spindel, J.E., Haibach, E. (1981) Some considerations in the statistical determination of the shape of S-N curves. In: *Statistical Analysis of Fatigue Data*, ASTM STP 744 (Edited by Little, R. E. and Ekvall, J. C.), pp. 89–113.
- [49] Hertzberg, R. W. (1996) *Deformation and Fracture Mechanics of Engineering Materials*. 4th Edition, Chichester, Wiley, New York, USA.
- [50] Xiaoguang, Y., Jia, H., Duoqi, H., Xiaoan, H., Chengli, D. (2013) LCF behavior and life modeling of DZ125 under complicated load condition at high temperature. In: *Proceedings of 13th International Conference on Fracture*, Beijing, China, June 16–21, 2013.
- [51] Lazzarin, P., Tovo, R. (1996) A unified approach to the evaluation of linear elastic stress fields in the neighbourhood of cracks and notches. *Int. J. Fracture* **78**, 3-19.

- [52] Yokobori, A.T., Kaji, Y., Kuriyama, T. (2001) Damage Progression Behavior under High Temperature Creep and Fatigue Conditions. In: *Proc. of the 10th International Conference on Fracture (ICF10)*, Paper n. ICF100882OR, Hawaii, USA, December 2-6, 2001 (available at: www.gruppofrattura.it).
- [53] Dowling, N. E. (1993) *Mechanical behaviour of materials: Engineering methods for deformation, fracture and fatigue*. Prentice-Hall, New Jersey, USA. ISBN-13: 978-0139057205.
- [54] Jones, R., Molent, L., Barter, S. (2013) Calculating crack growth from small discontinuities in 7050-T7451 under combat aircraft spectra. *Int. J. Fatigue* **55**, 178-182.
- [55] Lazzarin, P. and Zamabardi, R. (2002) The equivalent strain energy density approach reformulated and applied to sharp V-shaped notches under localized and generalized plasticity. *Fatigue Fract. Engng. Mater. Struct.* **25**, 917–928.

List of Captions

- Table 1.** Summary of the results generated by testing, at $T=250^{\circ}\text{C}$, plain and notched samples of C45; accuracy of the TCD applied in the form of the PM, LM, and AM.
- Table 2.** Summary of the results generated by Chen et al. [16] by testing, at $T=500^{\circ}\text{C}$, notched cylindrical samples of Inconel 718; accuracy of the TCD applied in the form of the PM, LM, and AM.
- Table 3.** Summary of the results generated by Shi et al. [19] by testing, at $T=850^{\circ}\text{C}$, notched cylindrical samples of directionally solidified superalloy DZ125; accuracy of the TCD applied in the form of the PM, LM, and AM.
- Figure 1.** Local system of coordinates (a); The Theory of Critical Distances formalised according to the Point (b), Line (c), and Area Method (d).
- Figure 2.** Determination of the critical distance value by using two calibration fatigue curves.
- Figure 3.** Geometries of the tested samples (the dimensions in millimetres) (a); un-notched and notched samples of C45 showing evident fatigue cracks (b).
- Figure 4.** Testing apparatus and plain sample mechanically clamped inside the furnace.
- Figure 5.** Summary of the generated experimental results: Wöhler curves and associated scatter bands for $P_S=10\%$ and $PS=90\%$.
- Figure 6.** Linear-elastic stress distance curves at the endurance limit for structural steel C45 and determination of critical distance L .
- Figure 7.** Linear-elastic stress distance curves at the endurance limit for Inconel 718 [16] and determination of critical distance L .
- Figure 8.** Linear-elastic stress distance curves at the endurance limit for directionally solidified superalloy DZ125 [19] and determination of critical distance L .
- Figure 9.** Overall accuracy of the TCD applied in the form of the PM, LM, and AM.

Tables

Notch type	K_t	N. of samples	R	k	$\Delta\sigma_0^{(1)}$ [MPa]	$N_{Ref}^{(2)}$ [Cycles]	T_σ	$\Delta\sigma_{eff}$			Error		
								PM [MPa]	LM [MPa]	AM [MPa]	PM [%]	LM [%]	AM [%]
Plain	1.0	10		7.8	429.2		1.222	-	-	-	-	-	-
Blunt U-Notch	6.9	9	0.1	3.5	75.0	$5 \cdot 10^5$	1.300	471.0	436.4	476.6	9.7	1.7	11.1
Sharp U-Notch	10.0	9		3.4	55.2		1.496	439.8	380.0	449.1	2.5	-11.5	4.6
Sharp V-Notch	26.5	8		3.1	42.2		1.891	429.2	369.9	439.5	0.0	-13.8	2.4

⁽¹⁾Range of the nominal stress referred to the net area.

⁽²⁾ N_{Ref} taken equal to $5 \cdot 10^5$ cycles to failure according to Sonsino [46].

Table 1. Summary of the results generated by testing, at $T=250^\circ\text{C}$, plain and notched samples of C45; accuracy of the TCD applied in the form of the PM, LM, and AM.

w_g [mm]	w_n [mm]	r_n [mm]	K_t	$\Delta\sigma_{0,n}$ [MPa]	$\Delta\sigma_{eff}$			Error		
					PM [MPa]	LM [MPa]	AM [MPa]	PM [%]	LM [%]	AM [%]
9	8	1.00	2.0	460	787.3	709.5	800.0	10.9	-0.1	12.7
9	8	0.10	4.8	370	743.1	657.8	762.1	4.7	-7.4	7.3
9	8	0.05	6.7	370	718.1	668.0	748.7	1.1	-5.9	5.5
10	8	1.00	2.2	450	846.8	761.8	858.5	19.3	7.3	20.9
10	8	0.10	5.8	310	737.0	641.0	752.1	3.8	-9.7	5.9
10	8	0.05	8.0	310	710.0	650.2	747.6	0.0	-8.4	5.3

Table 2. Summary of the results generated by Chen et al. [16] by testing, at $T=500^\circ\text{C}$, notched cylindrical samples of Inconel 718; accuracy of the TCD applied in the form of the PM, LM, and AM.

Ref.	w_g	w_n	r_n	K_t	N. of samples	T	R	k	$\Delta\sigma_0^{(1,2)}$	T_σ	$\Delta\sigma_{eff}$			Error		
	[mm]	[mm]	[mm]			[°C]					PM	LM	AM	PM	LM	AM
[50]	10	10	-	1.0	11		0.05÷0.1	7.5	1210	1.147	-	-	-	-	-	-
[19]	6	5.4	0.4	3.4	9	850	0.1	13.1	823	1.460	1360.7	1227.3	1372.5	12.5	1.4	13.4
[19]	6	5.5	0.2	4.2	7		0.1	12.4	711	1.356	1058.4	1010.9	1092.3	-12.5	-16.5	-9.7
[19]	6	5.4	0.3	3.7	8		0.1	15.1	849	1.280	1372.3	1262.3	1398.3	13.4	4.3	15.6

⁽¹⁾Range of the nominal stress referred to the net area.

⁽²⁾Endurance limit extrapolated at $N_0=10^6$ cycles to failure.

Table 3. Summary of the results generated by Shi et al. [19] by testing, at $T=850^\circ\text{C}$, notched cylindrical samples of directionally solidified superalloy DZ125; accuracy of the TCD applied in the form of the PM, LM, and AM.

Figures

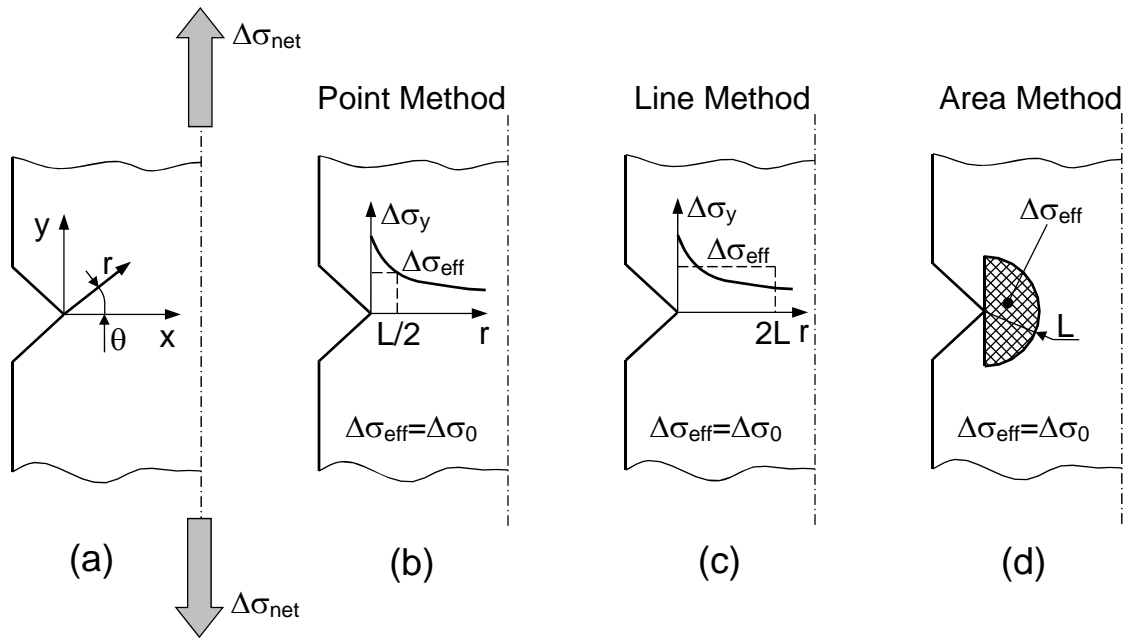


Figure 1. Local system of coordinates (a); The Theory of Critical Distances formalised according to the Point (b), Line (c), and Area Method (d).

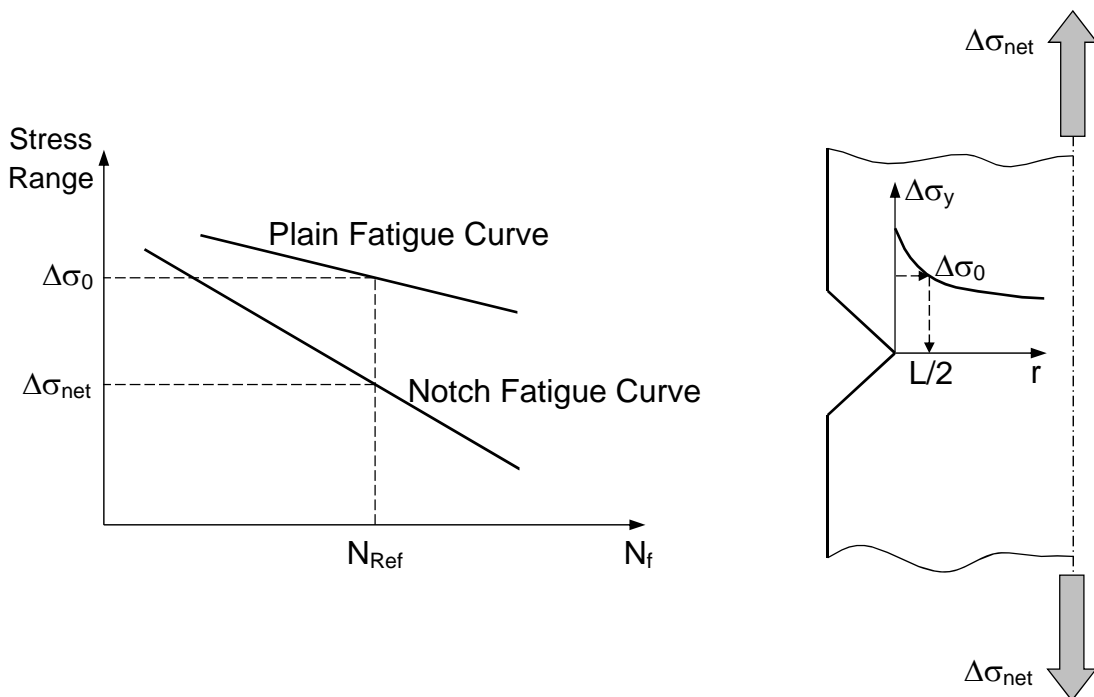
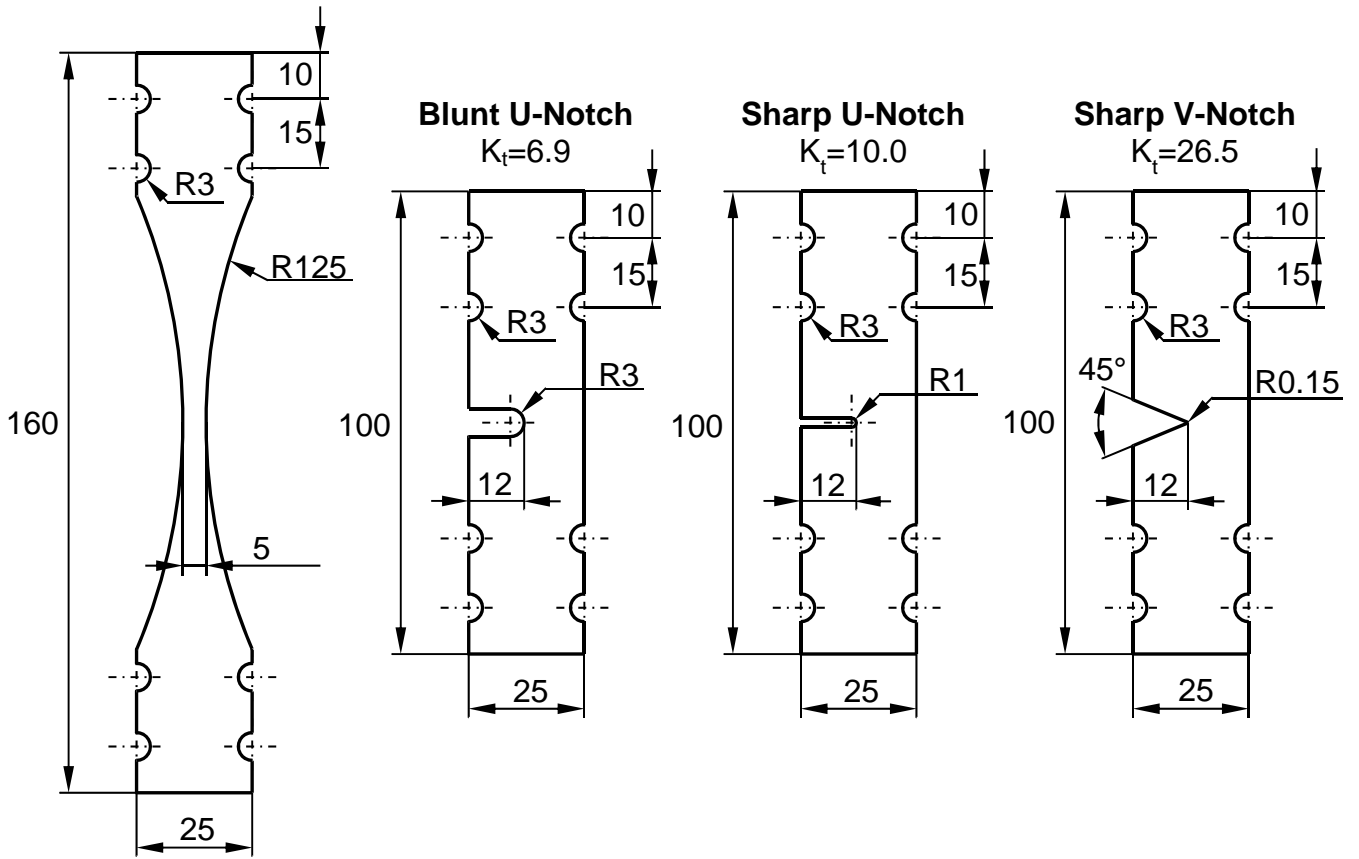


Figure 2. Determination of the critical distance value by using two calibration fatigue curves.



(a)



(b)

Figure 3. Geometries of the tested samples (dimensions in millimetres) (a); un-notched and notched samples of C45 showing evident fatigue cracks (b).

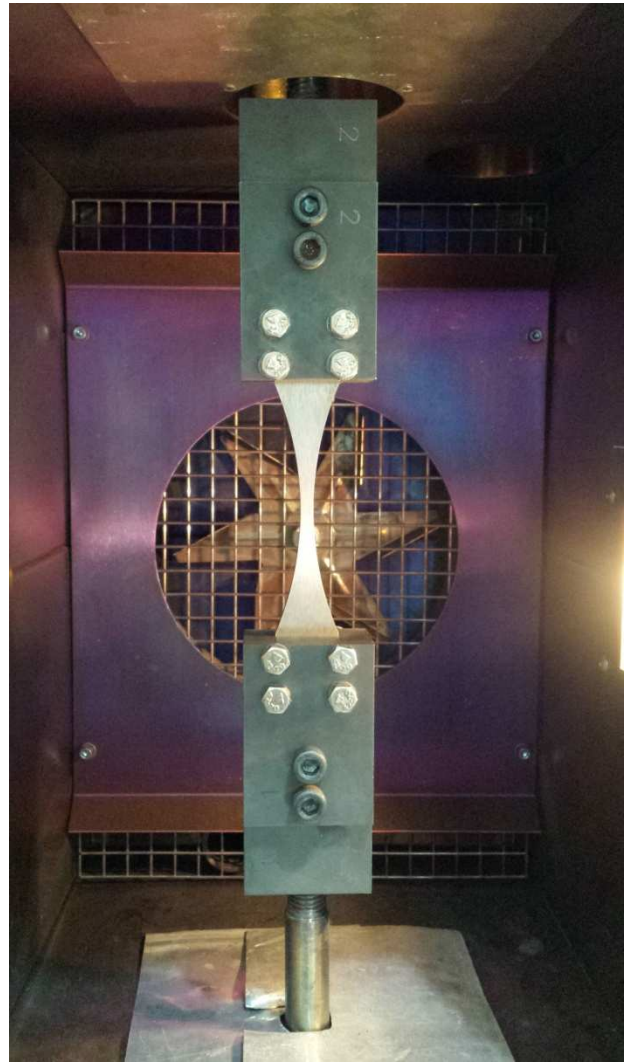
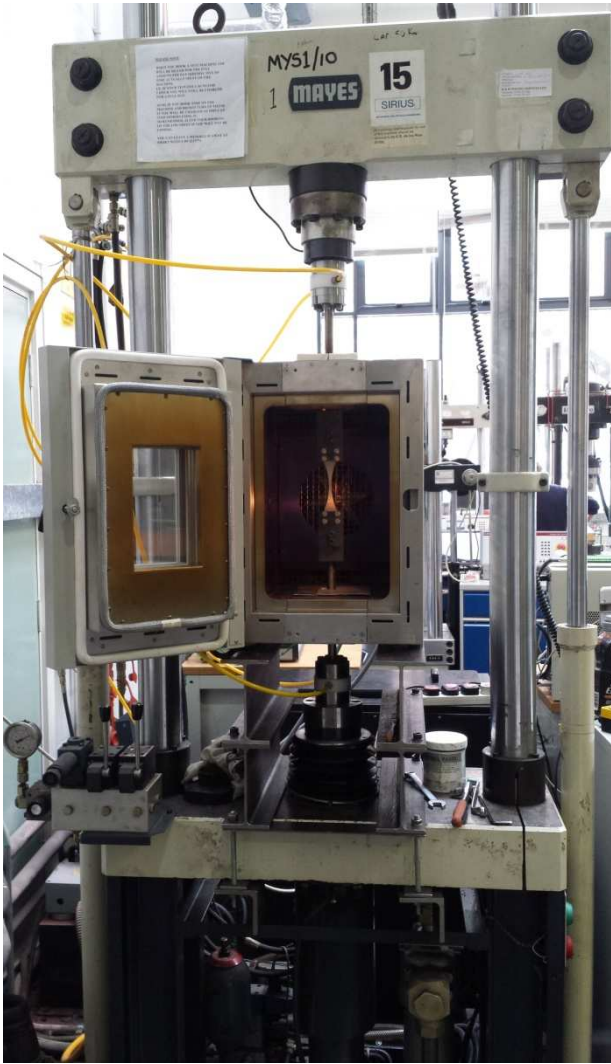


Figure 4. Testing apparatus and plain sample mechanically clamped inside the furnace.

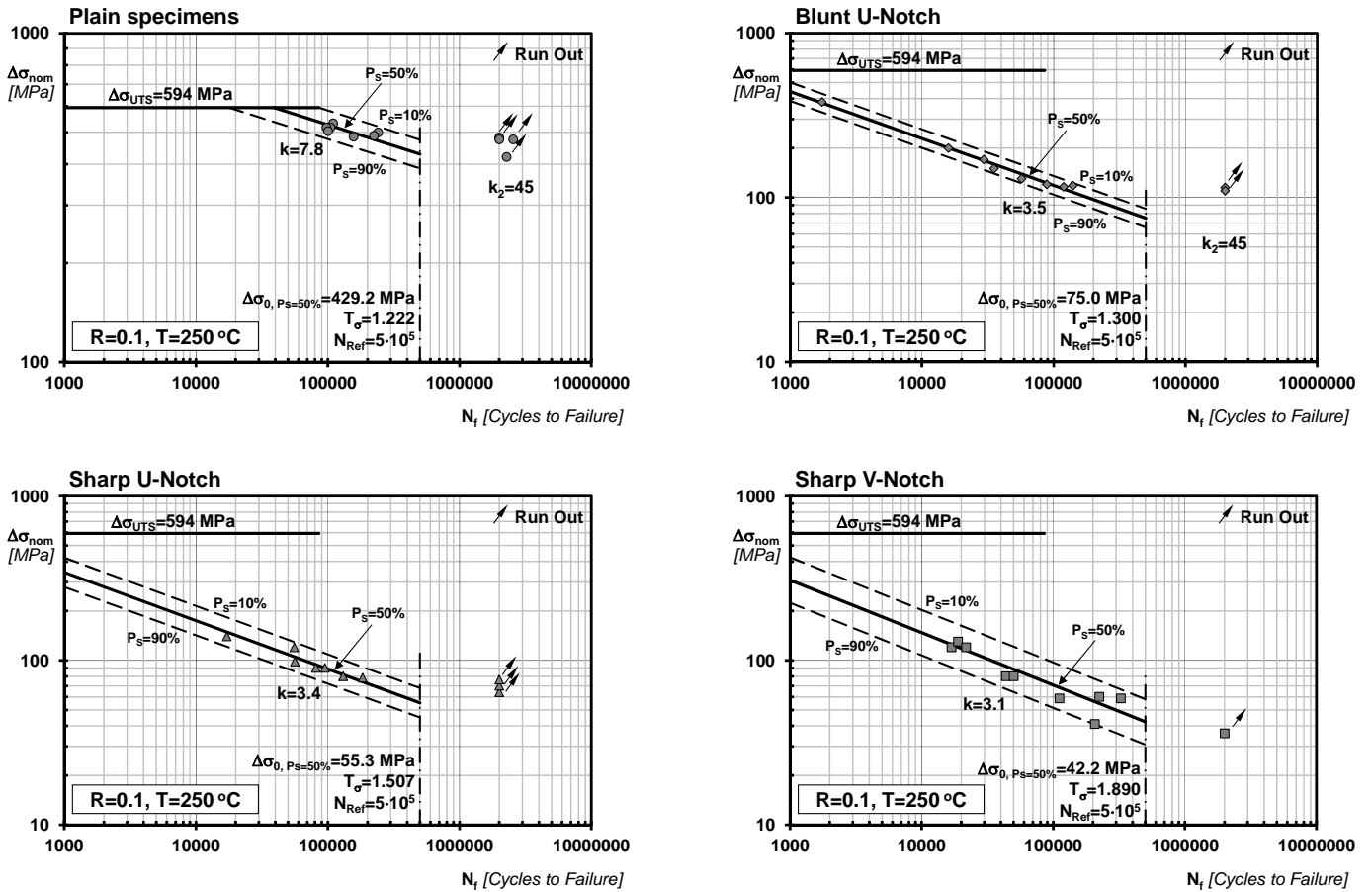


Figure 5. Summary of the generated experimental results: Wöhler curves and associated scatter bands for $P_S=10\%$ and $P_S=90\%$.

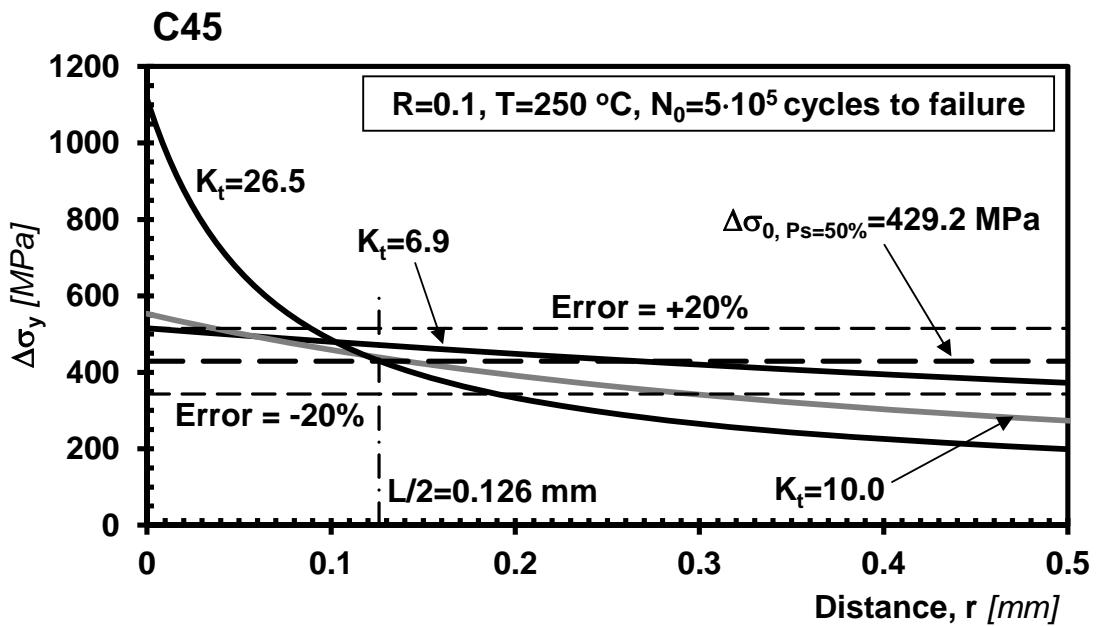


Figure 6. Linear-elastic stress distance curves at the endurance limit for structural steel C45 and determination of critical distance L .

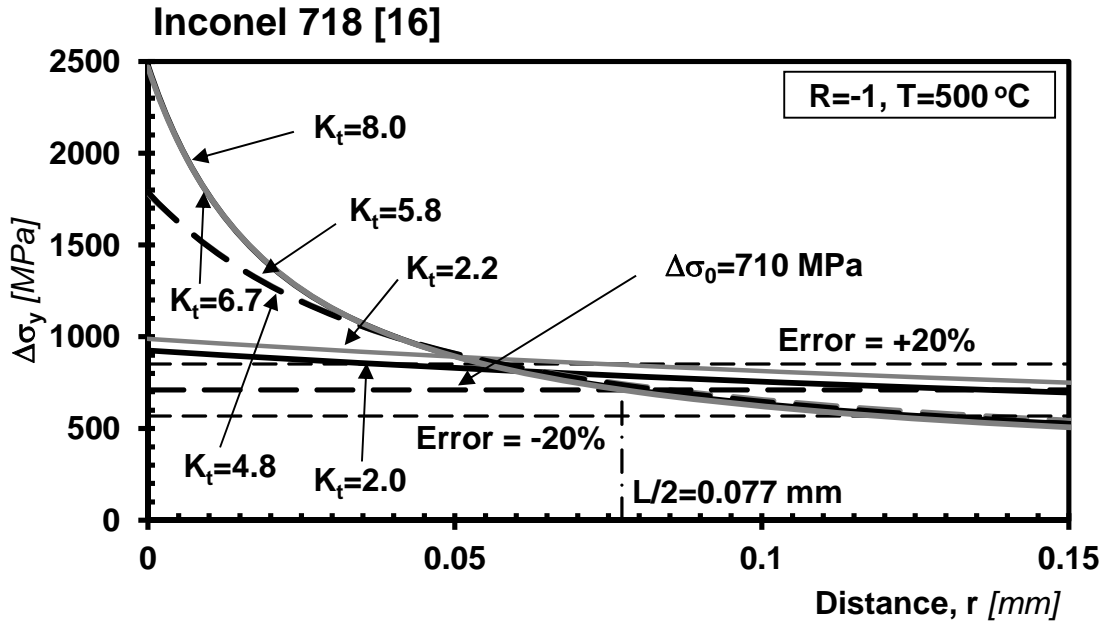


Figure 7. Linear-elastic stress distance curves at the endurance limit for Inconel 718 [16] and determination of critical distance L .

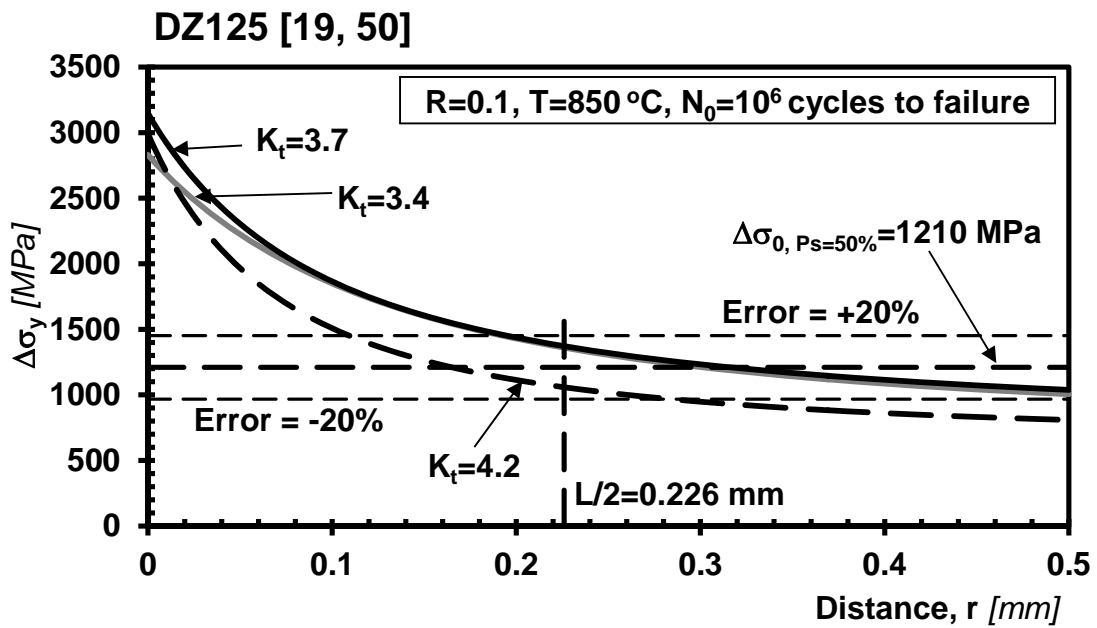


Figure 8. Linear-elastic stress distance curves at the endurance limit for directionally solidified superalloy DZ125 [19, 50] and determination of critical distance L .

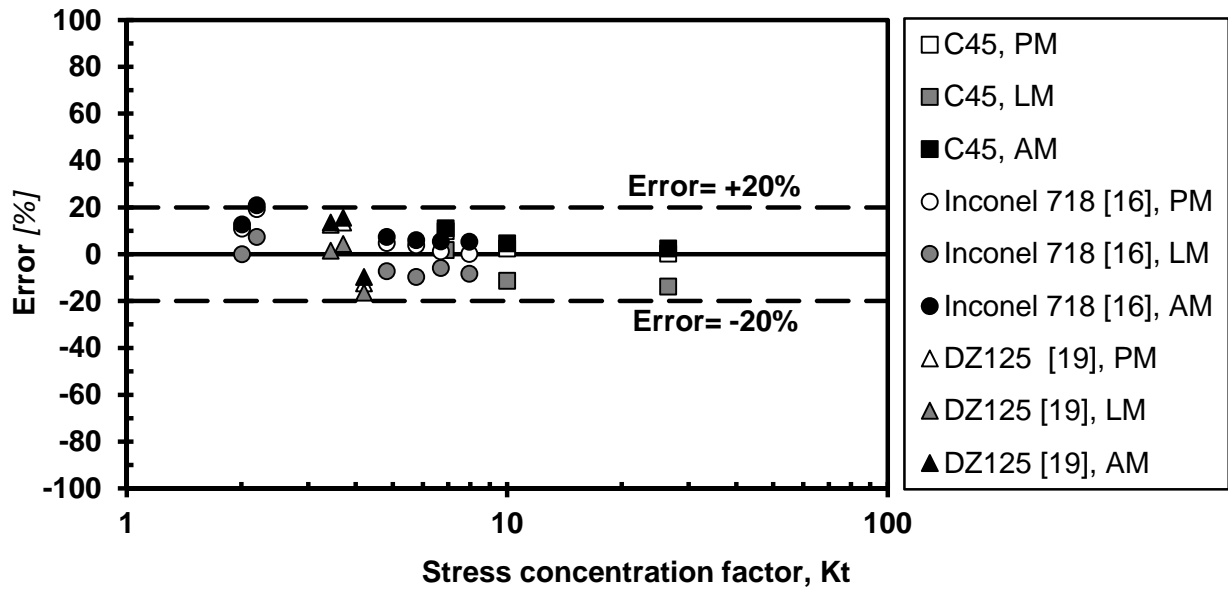


Figure 9. Overall accuracy of the TCD applied in the form of the PM, LM, and AM.